Chinese Chemical Letters 34 (2023) 107620

Contents lists available at ScienceDirect

Chinese Chemical Letters

journal homepage: www.elsevier.com/locate/cclet

Enhanced removal of phosphonates from aqueous solution using PMS/UV/hydrated zirconium oxide process

Shunlong Pan[a,b], Xi Nie[a], Xinrui Guo[a], Hao Hu[a], Biming Liu[c,*], Yongjun Zhang[a]

[a] School of Environmental Science and Engineering, Nanjing Tech University, Nanjing 210009, China
[b] College of Environment, Hohai University, Nanjing 210098, China
[c] State Key Joint Laboratory of Environment Simulation and Pollution Control, School of Environment, Tsinghua University, Beijing 100084, China

ARTICLE INFO

Article history:
Received 5 January 2022
Revised 7 April 2022
Accepted 18 June 2022
Available online 22 June 2022

Keywords:
Phosphonates
Peroxymonosulfate
UV
ROS
Adsorption

ABSTRACT

Traditional treatment processes cannot completely remove phosphonates in circulating cooling water by one-step method. Herein, we designed peroxymonosulfate/UV irradiation/hydrated zirconium oxide (PMS/UV/HZO) coupling process to enhance the phosphonates removal. In particular, nitrilotrismethylenephosphonic acid (NTMP) removal efficiency by PMS/UV/HZO process was much higher than that of PMS/UV process, UV/HZO process and other processes in comparison experiments. Specifically, almost 97.2% NTMP in water was degraded, and the total phosphorous (TP) reduced from 9.3 mg/L to 0.26 mg/L at pH 7 within 180 min. TP removal efficiency still reached above 90% after 5 cycles adsorption-desorption of HZO. Moreover, Cl^-, NO_3^- and SO_4^{2-} ions all had negligible effect on NTMP removal. During the process, NTMP was first destroyed to form phosphates and other intermediates by the reactive oxygen species (ROS), then phosphates were *in situ* immobilized *via* HZO adsorption. Sulfate radical ($SO_4^{\bullet-}$) has been confirmed to be the major ROS in the reaction system by quenching experiment and electron paramagnetic resonance (EPR) characterization. And the excellent selective adsorption capacity of HZO for phosphate produced was attributed to the strong inner-sphere coordination between $H_2PO_4^-$/HPO_4^{2-} and Zr-OH on the surface of HZO. These results suggest that PMS/UV/HZO process is a promising technique for enhanced phosphonates decontamination.

Phosphonates containing C-$PO(OH)_2$ group are important synthetic complexing agents, which have the characteristics of strong complexation stability, high water solubility, poor oil solubility and weak volatility [1]. Thus, phosphonates are widely used for scale and corrosion inhibition of industrial circulating cooling water system [2]. And the concentration of phosphonates in the wastewater can reach 1.5–20 mg/L [3]. However, phosphonates are easily photodegraded into cytogenotoxic aminomethyl phosphate (AMPA) and phosphate, which leads to the eutrophication of water bodies [4]. Thus, the advanced removal of phosphonates is an urgent need in the field of water-pollution control.

Traditional treatment processes have been employed to remove phosphonates from aqueous solution, including biodegradation, adsorption and coagulation/precipitation [5]. Unfortunately, biodegradation cannot effectively remove phosphonates due to the strong stability of C–P bonds in the molecular structure [6]. Adsorbents have a low adsorption capacity for phosphonates in neutral and weakly alkaline solutions [7]. Metal ions in coagulation/precipitation regents can be chelated with phosphonates, resulting in high consumption of chemical agents [8]. Recently, advanced oxidation processes (AOPs) have been used to effectively degrade phosphonates through reactive oxygen species (ROS), and then the remaining phosphates would be removed through coagulation/precipitation process [9]. Notably, sulfate radical ($SO_4^{\bullet-}$) based AOPs (SR-AOPs) have attracted extensive interest due to the potential for degrading organic contaminant in water [10]. Peroxymonosulfate (PMS) has the characteristics of stable properties, low cost, high water solubility and easy storage at room temperature, so it is favored in environmental remediation applications [11]. Activated by transition metals, ultraviolet (UV), heat or electron conduction, PMS can produce abundant $SO_4^{\bullet-}$ and hydroxyl radicals ($^{\bullet}OH$) [12]. Among them, using UV radiation to destroy chemical bonds to activate PMS is a benign and economical method. Compared with H_2O_2/UV process, PMS/UV process was more efficient for the removal of persistent contaminants [13]. Because the photolysis rate of H_2O_2 to produce ROS was much lower than that of PMS. Moreover, $SO_4^{\bullet-}$ has higher oxidation potential ($E_0 = 2.5$–3.1 V), wider reaction pH range (2–8), and longer half-life period

* Corresponding author.
E-mail address: bimingliu@tsinghua.edu.cn (B. Liu).

https://doi.org/10.1016/j.cclet.2022.06.043
1001-8417/

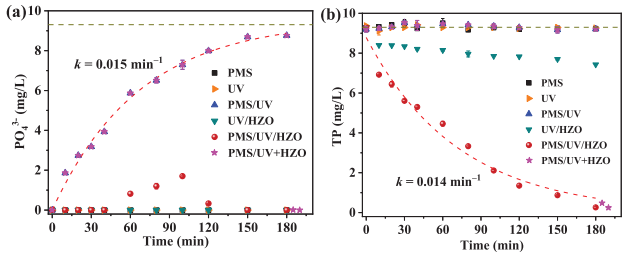

Fig. 1. (a, b) Effect of different processes on NTMP removal (25 °C, $[NTMP]_0 = 0.1$ mmol/L (9.3 mg TP/L), $[PMS]_0 = 1.5$ mmol/L, HZO = 0.8 g/L, pH_0 7, $UV_{254} = 0.045$ mW/cm^2).

(30–40 μs) than •OH [14]. But $SO_4^{\bullet-}$ would be consumed by accumulated phosphates, resulting in a certain reduction in reaction efficiency.

Hydrated zirconium oxide (HZO) has attracted more and more attention because of its excellent adsorption capacity for phosphates [15]. HZO is an amphoteric compound formed by the combination of amorphous Zr with water, which has strong acid and alkaline resistance [16]. Abundant hydroxyl groups distribute on the surface of HZO, which enables HZO to have great selective removal ability for phosphates by inner-sphere complexation [17]. Furthermore, the exhausted HZO also possesses great reusability. Compared with the coagulation/precipitation method, the advanced removal of phosphates by HZO could effectively reduce the eutrophication of receiving waterbody, and avoid the loss of phosphorus resource as well as reduce the trouble of sludge [18]. Recently, PMS/UV process has been adopted to degrade phosphonates in water, but the removal efficiency of innovative PMS/UV/HZO process for phosphonates is still unknown and needs further exploration. Additionally, current research is mainly for lab-scale simulated wastewater with a single contaminant, and complex water environment for phosphonates removal needs to be considered simultaneously.

In this study, we verified the advanced removal efficiency of phosphonates through the PMS/UV/HZO process. For this purpose, nitrilotris-methylenephosphonic acid (NTMP) was employed as the target pollutant. In order to confirm the availability of PMS/UV/HZO process, different treatment processes were firstly investigated. The effects of representative parameters on NTMP removal efficiency were optimized, such as initial pH, PMS concentration, HZO dose, NTMP concentration. Then, the existing ROS and the removal mechanism of NTMP were explored and revealed.

Reagents and chemicals are provided in Text S1 (Supporting information). HZO was prepared by the specific sol-gel method (Text S2 in Supporting information). Additionally, the relevant experimental procedures and analytical methods are shown in Text S3 (Supporting information). In the PMS/UV system, NTMP was efficiently oxidized to phosphates, and the formation of phosphate followed the *pseudo*-first-order kinetic model ($R^2 > 0.99$) (Fig. 1a). 94.2% of total phosphorous (TP) was finally converted to phosphate at pH 7 within 180 min. However, the generation of phosphates was negligible under the condition of PMS or UV alone. It was attituded to the fact that NTMP degradation caused by generated ROS under the effect of PMS photolysis, rather than by the direct photolysis of NTMP or the chemical oxidation of PMS [5]. The amount of phosphates produced in the PMS/UV/HZO process is significantly lower than the PMS/UV process, which was caused by HZO adsorption, and it was confirmed that NTMP degradation reaction and phosphates adsorption process occurred simultaneously. Surprisingly, the amount of phosphates in the solution increased first and then decreased during the PMS/UV/HZO process, and the concentration is as high as 1.7 mg/L at 100 min. This may be due to the excess phosphates produced by ROS at the early stage of reaction, which made the production rate of phosphates higher than adsorption rate of HZO, so that the concentration of phosphates rose [17]. Subsequently, the ROS in the later stage of reaction gradually decreased, and the phosphates concentration produced by degradation also gradually decreased. The production rate of phosphates was lower than adsorption rate, resulting in a decrease in phosphates concentration. When PMS/UV/HZO process was divided into two steps: PMS/UV oxidation (180 min) and HZO adsorption (10 min), TP concentration reduced to 0.25 mg/L, achieving the same effect as combined process. In contrast, if the process was carried out separately, the step was fussy and the cost was high. On the other hand, TP was significantly removed in PMS/UV/HZO system (Fig. 1b), and TP removal efficiency followed the pseudo-first-order kinetic model ($R^2 > 0.97$). All the phosphates generated was removed by ROS and HZO adsorption within 180 min, so that 97.2% of TP could be effectively removed. But TP was only slightly removed under HZO/UV condition. The dramatic difference demonstrated that phosphates instead of NTMP could be well selectively adsorbed by HZO.

ROS quenching experiment is an efficient strategy to verify the existence of ROS. Ethanol (EtOH) was used as the scavenger of •OH (k(•OH) = 9.1 × 10^6 L mol^{-1} s^{-1}) and $SO_4^{\bullet-}$ ($k(SO_4^{\bullet-})$ = 3.5 × 10^7 L mol^{-1} s^{-1}), and tertiary butanol (TBA) was used as the scavenger of •OH (k(•OH) = (3.8–7.6) × 10^8 L mol^{-1} s^{-1}) [19]. As shown in Fig. S1a (Supporting information), after adding 5 mmol/L TBA to the system, TP removal efficiency decreased to 83.9%, and k_{obs} was 0.035 min^{-1}. Continuing to increase TBA dosage to 20 mmol/L, TP removal efficiency and k_{obs} nearly unchanged, demonstrating that excess TBA has completely quenched •OH in the system. Similarly, adding 2 or 5 mmol/L EtOH to the system, TP removal efficiency continued decreasing to ~45.2% (Fig. S1b in Supporting information). The above results indicate that both $SO_4^{\bullet-}$ and •OH exist in the system, and some other ROS (such as singlet oxygen radicals ($^1O_2$), superoxide anion radicals ($O_2^{\bullet-}$)) may involve in the degradation process of NTMP. Therefore, NaN_3 and *p*-benzoquinone (*p*-BQ) were also used as quenchers to measure whether $^1O_2$ and $O_2^{\bullet-}$ existed in the system, respectively. NaN_3 can effectively quench $^1O_2$, •OH and $SO_4^{\bullet-}$. The addition of excess NaN_3 further decreased TP removal efficiency to 30.1% (Fig. S1c in Supporting information). Surprisingly, with the addition of 20 mmol/L *p*-BQ, TP removal efficiency slightly reduced to 78.5%, and k_{obs} was 0.032 min^{-1} (Fig. S1d in Supporting information). This confirms that $SO_4^{\bullet-}$, •OH, $^1O_2$ and $O_2^{\bullet-}$ exist in the system, and $SO_4^{\bullet-}$ is the major ROS in NTMP degradation according to the quenching results of different quenchers.

ROS were further identified by EPR characterization (Fig. 2). The characteristic signal with a peak strength ratio of 1:2:2:1 belonged to DMPO-•OH, indicating that •OH existed in the reaction solution [20]. The peak signal of DMPO-$SO_4^{\bullet-}$ (α_N = 13.9 G, α_H = 9.9 G, α_H = 0.9 G, α_H = 0.6 G) is observed near the •OH signal, implying the existence of $SO_4^{\bullet-}$ (Fig. 2a). Besides, DMPO also detected the peak of $O_2^{\bullet-}$ (Fig. 2b). Use TEMP as a spin trapping agent to directly verify the existence of $^1O_2$ by forming TEMPO, which is a typical triplet (intensity ratio = 1:1:1) (Fig. 2c). Moreover, it can be seen that the peak intensities of all peaks at 5 min are higher than 2 min. Results revealed that the number of ROS increased gradually with reaction time, and the reaction became more intense. EPR results are consistent with the results of quenching experiment. In summary, both radical and non-radical ROS exist in the catalytic system.

Based on the above analysis about ROS, the generation pathway of ROS in the system was proposed. $SO_4^{\bullet-}$ and •OH were first generated by UV activation of PMS, and then $SO_4^{\bullet-}$ could react with H_2O to continue to generate •OH (Eqs. 1 and 2) [21]. In addition, UV could provide electrons to O_2 alone to generate $O_2^{\bullet-}$ (Eq. 3),

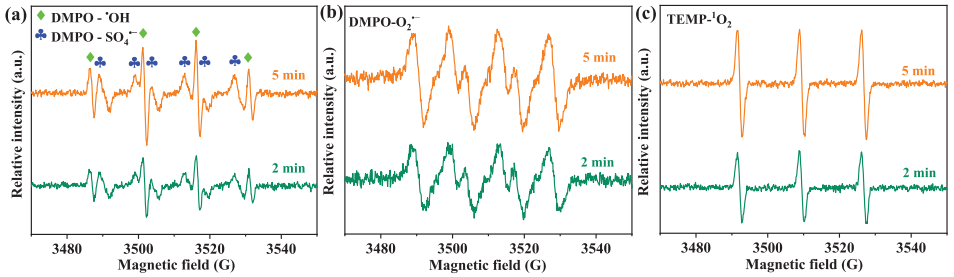

Fig. 2. (a–c) EPR spectra of different systems in NTMP solution (25 °C, $[NTMP]_0 = 0.1$ mmol/L (9.3 mg TP/L), $[PMS]_0 = 1.5$ mmol/L, HZO = 0.8 g/L, pH_0 7, $UV_{254} = 0.045$ mW/cm^2).

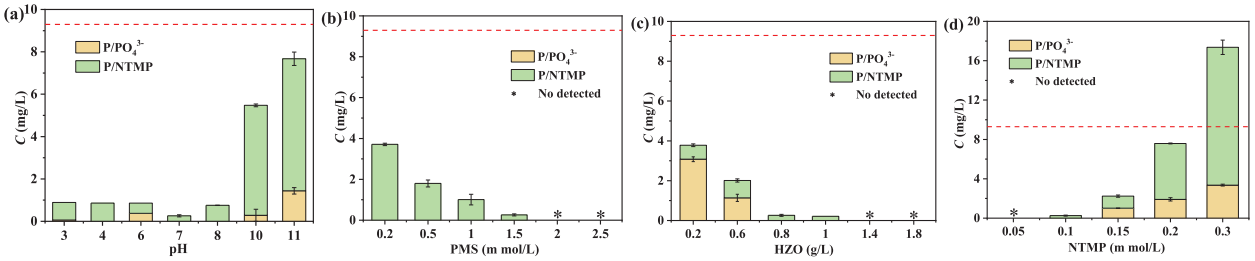

Fig. 3. NTMP removal in different conditions (a) pH_0 value (25 °C, $[NTMP]_0 = 0.1$ mmol/L (9.3 mg TP/L), $[PMS]_0 = 1.5$ mmol/L, HZO = 0.8 g/L, $UV_{254} = 0.045$ mW/cm^2); (b) PMS concentration (25 °C, $[NTMP]_0 = 0.1$ mmol/L (9.3 mg TP/L), HZO = 0.8 g/L, pH_0 7, $UV_{254} = 0.045$ mW/cm^2); (c) HZO dose (25 °C, $[NTMP]_0 = 0.1$ mmol/L (9.3 mg TP/L), $[PMS]_0 = 1.5$ mmol/L, pH_0 7, $UV_{254} = 0.045$ mW/cm^2) and (d) NTMP concentration (25 °C, $[PMS]_0 = 1.5$ mmol/L, HZO = 0.8 g/L, pH_0 7, $UV_{254} = 0.045$ mW/cm^2).

and ·OH could generate $^1O_2$ through disproportionation (Eq. 4) [22]. $SO_5^{\bullet-}$ in the reaction could also react with H_2O to generate $^1O_2$ (Eq. 5) [23]. Thus, NTMP molecules were effectively degraded under the synergistic effect of radicals and non-radicals (Eq. 6).

$$HSO_5^- \xrightarrow{UV} SO_4^{\bullet-} + {}^{\bullet}OH \quad (1)$$

$$SO_4^{\bullet-} + H_2O \rightarrow SO_4^{2-} + {}^{\bullet}OH + H^+ \quad (2)$$

$$O_2 \xrightarrow{UV} O_2^{\bullet-} \quad (3)$$

$$4{}^{\bullet}OH \rightarrow {}^1O_2 + 2H_2O \quad (4)$$

$$2SO_5^{\bullet-} + H_2O \rightarrow 2HSO_4^- + 1.5\,{}^1O_2 \quad (5)$$

$$SO_4^{\bullet-} + {}^1O_2 + NTMP \rightarrow \text{by-products} + CO_2 + H_2O \quad (6)$$

The distribution of ROS and the adsorption mechanism of HZO were greatly influenced by pH value [5]. As shown in Fig. 3a, TP removal efficiency varies between 17.4% and 97.2% with pH increasing from 3 to 10. Nevertheless, the removal efficiency suddenly decreases to 17.4% at strongly basic condition (pH 11). It was reported that the pK_{a1} and pK_{a2} of PMS were 0 and 9.4, respectively [24]. Thus, the main existence form of PMS was HSO_5^- when pH was lower than 9.4, while SO_5^{2-} appeared at pH > 9.4. In addition, the dominant ROS was $SO_4^{\bullet-}$ in the acidic condition, and ·OH in the basic condition. But the standard reduction potential of ·OH was 1.8 V in neutral and basic solutions, lower than that of 2.7 V in acidic solution [25]. As shown in Fig. S2a (Supporting information), NTMP removal efficiency is particularly low in basic condition due to the weaker oxidation capacity and the shorter life span ($t_{1/2}$ < 1 μs) of dominant ·OH [26]. On the other hand, the surface properties of HZO could also be changed by the pH of solution, thus affecting the adsorption efficiency of phosphates. Fig. S2b (Supporting information) shows that the adsorption capacity of phosphates increases gradually as the pH of solution decreases. The higher adsorption capacity at a lower pH might be due to the fact that the hydroxyl groups on the HZO surface became protonated and positively charged at a pH lower than the isoelectric point [27]. As shown in Fig. S3 (Supporting information), the pH_{PZC} value of HZO is 5.6. When pH was greater than 5.6, the zeta potential of HZO gradually tended to be negative. Anions such as phosphates were more easily adsorbed by HZO in acidic and neutral pH solutions. Thus, the negatively charged phosphates ions were predominately adsorbed on the surface of adsorbent. The surface of HZO was negatively charged because of the deprotonation of surface hydroxyl groups at a higher pH value. Due to the Donnan co-ion exclusion or electrostatic repulsion, negatively charged phosphates ions could not be adsorbed by negatively charged HZO surface at higher pH, while favoring the desorption of HZO after phosphate adsorption [27].

PMS concentration will affect the generation and scavenging of $SO_4^{\bullet-}$ and ·OH, thus affecting NTMP removal efficiency. TP removal efficiency increases from 60% to 100% with the rise of PMS concentration from 0.2 mmol/L to 2.5 mmol/L (Fig. 3b). In particular, TP removal efficiency is increased to 97.2% as PMS concentration is 1.5 mmol/L. And it could be attributed to the enhancement of ROS strength with the increase of PMS dose. However, when PMS concentration is further increased to 2.5 mmol/L, there occurs negligible change in the removal efficiency. And it is inferred that ROS could be eliminated by reacting with excess PMS and $SO_4^{\bullet-}$ [28]. Therefore, NTMP removal efficiency increased significantly with the rise of PMS concentration, but it was inhibited at a higher PMS concentration. Notably, the phosphate produced was totally removed under different PMS concentrations, indicating that PMS concentration had a negligible effect on the adsorption capacity of HZO.

HZO dose will affect the utilization of adsorption active sites, and the effect of HZO dose on NTMP removal is shown in Fig. 3c. Results show that TP removal efficiency increases from 59% to 100% as HZO dose rises from 0.2 g/L to 1.8 g/L. Specially, TP removal efficiency reaches 97.2% when the HZO dose is 0.8 g/L, and the concentration of the remaining phosphorus species is only 0.26 mg/L. As for the adsorption of NTMP by HZO, TP only decreases slightly when HZO dose reaches 1.8 g/L (Fig. S4 in Supporting information). Therefore, it shows that HZO had an excellent selective adsorp-

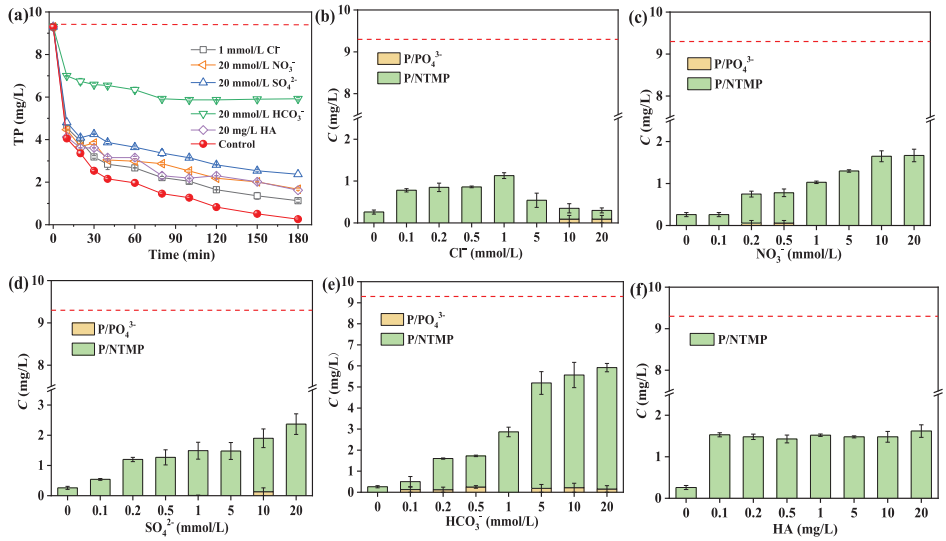

Fig. 4. Effect of the (a) coexisting substances on TP removal and the (b) Cl^-, (c) NO_3^-, (d) SO_4^{2-}, (e) HCO_3^- and (f) HA on NTMP removal (25 °C, pH_0 7, $[NTMP]_0 = 0.1$ mmol/L (9.3 mg TP/L), $[PMS]_0 = 1.5$ mmol/L, HZO = 0.8 g/L, $UV_{254} = 0.045$ mW/cm^2).

tion effect on phosphate rather than NTMP. The adsorption process could be divided into two stages: rapid adsorption and adsorption dynamic equilibrium [29]. Fresh HZO provided abundant active sites and promoted the diffusion and adsorption of phosphates. Then, almost all the active sites were occupied by phosphates, and the adsorption effect of adsorbent was dramatically reduced. With the increase of HZO dose, more active sites could be obtained to achieve the ideal NTMP removal efficiency.

Considering the practical application, the effect of NTMP concentration on NTMP removal efficiency was also studied (Fig. 3d). As a result that TP removal efficiency decreases from 100% to 38% with the increase of NTMP concentration from 0.05 mmol/L to 0.3 mmol/L. It was reported that NTMP had an internal filtering effect on the photolysis of PMS [5]. UV light in contact with PMS could be filtered by a higher concentration of NTMP, thereby reducing the generation of ROS. Additionally, $SO_4^{\bullet-}$ would also be consumed by accumulated phosphates, resulting in a decrease of degradation efficiency. Furthermore, evidence suggests that there existed a competitive adsorption between phosphates and phosphonate [30]. Thus the increase of NTMP concentration will inhibit the adsorption capacity of HZO for phosphates.

Cl^-, NO_3^-, SO_4^{2-} and HCO_3^- are ubiquitous coexisting anions in the industrial wastewater, which not only consume ROS, but also generate competitive adsorption with $H_2PO_4^-/HPO_4^{2-}$ on the HZO surface [29,31]. The order of inhibition intensity is $HCO_3^- > SO_4^{2-} > NO_3^- >$ HA $> Cl^-$ (Fig. 4a). Obviously, Cl^-, NO_3^- and SO_4^{2-} have negligible effect on NTMP removal (Figs. 4b–d). TP removal efficiency slightly decreases when the concentration of NO_3^- and SO_4^{2-} increases to 20 mmol/L. As for Cl^-, the removal efficiency first decreases and then increases. However, HCO_3^- shows a significant inhibitory effect, and TP removal efficiency decreases obviously from initial 97.2% to 36.3% (C = 20 mmol/L) (Fig. 4e).

It has been reported that Cl^- would consume $SO_4^{\bullet-}$ and $^{\bullet}OH$ generated by PMS photolysis, and generate $Cl^{\bullet}$ and secondary radicals containing Cl element ($Cl_2^{\bullet-}$ and $HOCl^{\bullet-}$) with lower redox potential ($E(Cl^{\bullet}/Cl^-) = 2.4$ V, $E(Cl_2^{\bullet-}/Cl^-) = 2.0$ V and $E(HOCl^{\bullet-}/Cl^-) = 1.48$ V) [32]. Gao *et al.* [33] found that the efficiency of thermally activated persulfate degradation of triclosan was inhibited by low concentration of Cl^- (< 10 mmol/L), but promoted by high concentration of Cl^- (20–50 mmol/L). The results also illustrate the dual effects of Cl^-, whose inhibition or enhancement were determined by the concentration (Fig. S5a in Supporting information). This might be attributed to the consumption of $SO_4^{\bullet-}$ and $^{\bullet}OH$ at a low concentration of Cl^-, thus reducing the oxidation efficiency. But a large amount of $Cl^{\bullet}$ and $Cl_2^{\bullet-}$ would produce because of a high concentration of Cl^-. Meanwhile, the reaction between Cl^- and $SO_4^{\bullet-}$ or $^{\bullet}OH$ was reversible (Eqs. 7 and 8), and could regenerate $SO_4^{\bullet-}$ or $^{\bullet}OH$ with high activity [31].

$$SO_4^{\bullet-} + Cl^- \leftrightarrow Cl^{\bullet} + SO_4^{2-}$$

$$k_{forward} = (2.47-6.6)\times 10^8\ L\,mol^{-1}\ s^{-1}, k_{backward} = 2.5\times 10^8\ L\,mol^{-1}\ s^{-1} \quad (7)$$

$$^{\bullet}OH + Cl^- \leftrightarrow HOCl^{\bullet-}$$

$$k_{forward} = 4.3\times 10^9\ L\,mol^{-1}\ s^{-1}, k_{backward} = 6.1\times 10^9\ L\,mol^{-1}\ s^{-1} \quad (8)$$

Different from the double action of Cl^- on oxidation process, NO_3^-, SO_4^{2-} and HCO_3^- only show inhibitory effects when they exist in the system. $SO_4^{\bullet-}$ and $^{\bullet}OH$ as the scavenger of radicals would react with NO_3^- to produce weaker active $NO_3^{\bullet}$ ($E = 2$–2.2 V) [34], thereby inhibiting PMS activation (Fig. S6a in Supporting information). It is found that the redox potential of $SO_4^{\bullet-}/SO_4^{2-}$ would be reduced by accumulated SO_4^{2-}, thus reducing the activation efficiency of PMS (Fig. S7a in Supporting information) [35]. As shown in Fig. S8a (Supporting information), $SO_4^{\bullet-}$ and $^{\bullet}OH$ would also be eliminated by HCO_3^-, and further produced $CO_3^{\bullet-}$ with poor oxidation efficiency [36]. In addition, the pH of solution would increase due to the strong buffering capacity of HCO_3^-, which reduced the oxidation potential of ROS, and also reduced the removal efficiency of target pollutant [31].

Excellent selective adsorption of HZO for $H_2PO_4^-/HPO_4^{2-}$ with the presence of coexisting anions was also studied. In the presence of different anions, the adsorption capacity of HZO was affected differently (Figs. S5b, S6b, S7b and S8b in Supporting information). The anions have different inhibitory intensity on phosphates adsorption, which in turn is $HCO_3^- > SO_4^{2-} > NO_3^- > Cl^-$. When the concentrations of Cl^-, NO_3^- and SO_4^{2-} were about 15, 30 and 60 times higher than that of NTMP, respectively, the adsorption capacity of HZO for phosphate decreased slightly. But HCO_3^- possessed the strong buffer capacity, which exerted the pH value high and the surface of HZO deprotonated, so phosphate adsorption was strongly inhibited. Generally, the adsorption efficiency of HZO for

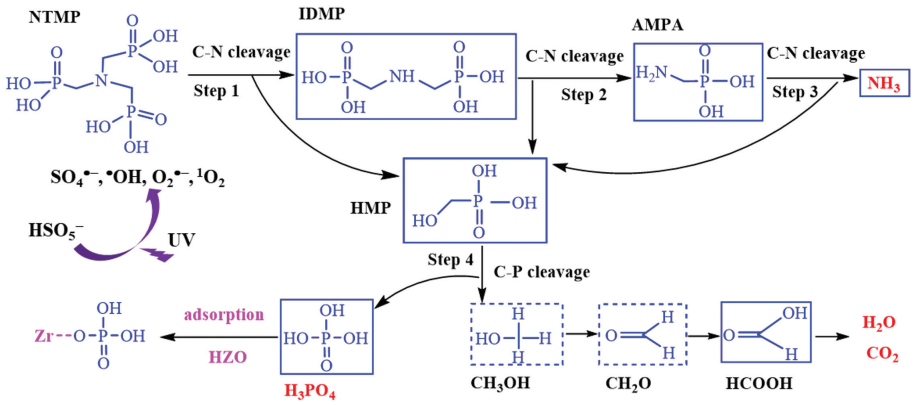

Fig. 5. Degradation pathway of NTMP by PMS/UV/HZO process.

phosphate decreased as the anion charge became higher [37]. Evidence also suggests that the inner-sphere complexation performed between SO_4^{2-} and HZO surface [29]. But weak outer-sphere complexation performed between Cl^-, NO_3^- and HZO surface, resulting in the ineffective competition [38].

Natural organic matter (NOM) is widely present in water bodies and usually has a certain negative effect on the removal of organic pollutants [39]. NTMP degradation efficiency decreases when the humic acid (HA) concentration is 0.1 mg/L (Fig. 4f). Interestingly, when HA concentration further increases, its inhibitory effect in the PMS/UV/HZO system is not further enhanced. Fig. S9a (Supporting information) illustrates that the presence of HA inhibits the degradation of NTMP in the PMS/UV process. It is speculated that the reaction between HA and $SO_4^{\bullet-}$ led to a decrease in oxidization ability. HA could compete for the adsorption sites of HZO by forming Zr-HA complexes, weakening phosphorus removal efficiency. But the increase in HA concentration had little effect on phosphate adsorption (Fig. S9b in Supporting information), presumably because larger HA molecules could not enter the internal pores of HZO [40].

As shown in Fig. S10 (Supporting information), NTMP removal efficiency in the simulated circulating cooling water is 91.0%, and the remaining TP is 0.84 mg/L, which indicates that the degradation effect of PMS/UV/HZO process on NTMP is slightly inhibited in the natural water environment. In general, the PMS/UV/HZO method, as a promising process, can be effectively applied to the removal of phosphonates in the actual industrial circulating cooling water. In order to verify the reuse performance of HZO, five cyclic adsorption/desorption experiment were conducted. TP removal efficiency still reaches above 90% after five cycles (Fig. S11 in Supporting information), thus proving that the adsorption process of HZO for phosphates was reversible.

NTMP is composed of three phosphonate groups (C-$PO(OH)_2$) and a central N atom. Intermediate products ((Iminodi (methylenephosphonic acid)) IDMP, AMPA and hydroxymethyl phosphonic acid (HMP)) were detected in by liquid chromatography-mass spectrometer (LC-MS) and results are showing in Fig. S12 and Table S1 (Supporting information). Furthermore, results show the TOC degradation rate (0.011 min^{-1}) is almost equal to the phosphates generation rate (0.015 min^{-1}) (Fig. S13 in Supporting information). NH_3-N was merely detected during the process while nitrate and nitrite were not detected, and N atoms in NTMP were eventually released in the form of NH_3-N (Fig. S14 in Supporting information). Compared with the rapid removal of TOC, the formation of NH_3-N has an obvious hysteresis effect. All the above evidences demonstrate that the C–N bond cleaved first and then C–P bond cleaved.

Based on the above analysis, NTMP degradation pathway was proposed (Fig. 5). One of the C–N bonds in NTMP molecule was cleaved to form IDMP and HMP after UV activation of PMS (Step 1) [5]. IDMP was further converted to AMPA and HMP (Step 2) [1]. Among them, AMPA was then oxidized to NH_3-N and HMP (Step 3) [5]. Subsequently, C-P bond in HMP molecule was cleaved to generate H_3PO_4 and methanol (CH_3OH) (Step 4) [5]. Moreover, since the ratio of $k_{obs\text{-}TOC}$ to $k_{obs\text{-}P}$ is close to 1, it indicates that methanol could be rapidly converted into formaldehyde (CH_2O) and formic acid (HCOOH) (Fig. S15 in Supporting information), as well as the mineralization products CO_2 and H_2O [5].

Some specific physicochemical analysis of HZO is provided in Text S4 (Supporting information). In order to determine the chemical composition and chemical state of adsorbent, the XPS spectra of HZO before and after phosphate adsorption were observed. It is found that a new peak belonging to phosphorus appears at the binding energy of 132.9 eV in the XPS wide spectra (Fig. S16 in Supporting information), which proved that phosphorus species were adsorbed by HZO. Fig. S17a (Supporting information) shows that the peak of Zr 3d can be fitted into four peaks, among which the peaks at 182.1 and 184.6 eV both belong to Zr–O bonds, and those at 182.8 and 186.0 eV belong to metallic Zr–Zr bonds [41]. The shift of the Zr–O binding energy after phosphates adsorption may be caused by Zr–O–P inner-sphere complexation structure formed between -Zr–OH and $H_2PO_4^-$/HPO_4^{2-} (Eq. 9) [17]. The three peaks of O 1s XPS spectra are corresponding to metals oxide (M–O), metal surface hydroxyl group (M–OH) and bound water (H_2O), respectively (Fig. S17b in Supporting information) [42]. And the percentage of M-O, M-OH and H_2O is 26.61%, 43.85%, and 29.54%, respectively. Analysis shows that the fraction of -Zr-OH/O-P component at 531.4 eV increased from 43.85% to 47.86% after phosphate adsorption, while the fraction of M–O at 529.9 eV decreased from 26.61% to 11.77%. This phenomenon further proved the formation of Zr–O–P bond after phosphate adsorption.

$$\text{Zr-(OH)}_y + bH_xPO_4^{(3-y)-}(aq) \rightarrow \text{Zr-(OH)}_{y-b}\left[H_xPO_4^{(3-x)-}\right]_b + bOH^-(aq) \quad (9)$$

In conclusion, PMS/UV/HZO treatment process has been applied for NTMP removal in water. Excess ROS contributed to NTMP degradation in neutral solution, so that PMS/UV process had the best oxidation effect at pH 7. And the higher adsorption capacity at a lower pH might be due to the fact that the hydroxyl groups on the HZO surface became protonated and positively charged at a pH lower than the isoelectric point. NTMP removal efficiency in the simulated circulating cooling water is 91.0%, and the remaining TP is 0.84 mg/L, which indicates that the degradation effect of

PMS/UV/HZO process for NTMP is slightly inhibited in the natural water environment. Under UV photolysis PMS, NTMP degradation began with the cleavage of C–N and C–P bonds, forming intermediate products, and finally mineralized into phosphates, NH_3-N and CO_2. According to EPR analysis and ROS quenching results, it can be confirmed that $SO_4^{\bullet-}$ played a major role in the NTMP removal.

Declaration of competing interest

All authors declared that they do not have any commercial and associative interests that represent a conflict of interest in connection with the other work submitted

Acknowledgments

The authors would like to express gratitude to the National Natural Science Foundation of China (No. 52000102) and the Natural Science Foundation of Jiangsu Province (No. BK20190689) for offering financial support to this research.

Supplementary materials

Supplementary material associated with this article can be found, in the online version, at doi:10.1016/j.cclet.2022.06.043.

References

[1] S. Sun, S. Wang, Y. Ye, B. Pan, Water Res. 153 (2019) 21–28.
[2] E. Rott, R. Minke, U. Bali, H. Steinmetz, Water Res. 122 (2017) 345–354.
[3] S. Wang, S. Sun, C. Shan, B. Pan, Water Res. 161 (2019) 78–88.
[4] X. Zhang, J. Li, W.Y. Fan, G.P. Sheng, Environ. Sci. Technol. 53 (2019) 4997–5004.
[5] Z. Wang, G. Chen, S. Patton, et al., Water Res. 159 (2019) 30–37.
[6] Q. Wang, Y. Shao, N. Gao, et al., Chem. Eng. J. 304 (2016) 201–208.
[7] R. Altaf, X. Lin, M.A. Tadda, S. Zhu, D. Liu, J. Clean. Prod. 278 (2021) 123960.
[8] E. Rott, M. Nouri, C. Meyer, et al., Water Res. 145 (2018) 608–617.
[9] E. Rott, R. Minke, H. Steinmetz, J. Water Process Eng. 17 (2017) 188–196.
[10] Y. Liu, X. He, Y. Fu, D.D. Dionysiou, J. Hazard. Mater. 305 (2016) 229–239.
[11] S. Wacławek, H.V. Lutze, K. Grübel, et al., Chem. Eng. J. 330 (2017) 44–62.
[12] Y.H. Guan, J. Ma, X.C. Li, J.Y. Fang, L.W. Chen, Environ. Sci. Technol. 45 (2011) 9308–9314.
[13] X. Zhang, J. Yao, Z. Zhao, J. Liu, Chem. Eng. J. 364 (2019) 1–10.
[14] P. Hu, M. Long, Appl. Catal. B: Environ. 181 (2016) 103–117.
[15] B. Pan, Z. Li, Y. Zhang, et al., Chem. Eng. J. 248 (2014) 290–296.
[16] Y. Su, H. Cui, Q. Li, S. Gao, J.K. Shang, Water Res. 47 (2013) 5018–5026.
[17] L. Fang, B. Wu, I.M.C. Lo, Chem. Eng. J. 319 (2017) 258–267.
[18] D.P. Van Vuuren, A.F. Bouwman, A.H.W. Beusen, Glob. Environ. Chang. 20 (2010) 428–439.
[19] T. Zeng, X. Zhang, S. Wang, H. Niu, Y. Cai, Environ. Sci. Technol. 49 (2015) 2350–2357.
[20] X. Liu, F. Huang, Y. Yu, et al., Appl. Catal. B: Environ. 253 (2019) 149–159.
[21] G.X. Huang, C.Y. Wang, C.W. Yang, P.C. Guo, H.Q. Yu, Environ. Sci. Technol. 51 (2017) 12611–12618.
[22] Q. Yi, J. Ji, B. Shen, et al., Environ. Sci. Technol. 53 (2019) 9725–9733.
[23] Y. Gao, Y. Zhu, L. Lyu, et al., Environ. Sci. Technol. 52 (2018) 14371–14380.
[24] J. Liu, J. Zhou, Z. Ding, et al., Ultrason. Sonochem. 34 (2017) 953–959.
[25] C. Liu, L. Liu, X. Tian, et al., Appl. Catal. B: Environ. 255 (2019) 117763.
[26] W.D. Oh, Z. Dong, T.T. Lim, Appl. Catal. B: Environ. 194 (2016) 169–201.
[27] A. Sarkar, S.K. Biswas, P. Pramanik, J. Mater. Chem. 20 (2010) 4417–4424.
[28] S. Khan, X. He, J.A. Khan, et al., Chem. Eng. J. 318 (2017) 135–142.
[29] M. Li, B. Zhang, S. Zou, Q. Liu, M. Yang, J. Hazard. Mater. 384 (2020) 121386.
[30] B. Nowack, A.T. Stone, Water Res. 40 (2006) 2201–2209.
[31] S. Xiao, M. Cheng, H. Zhong, et al., Chem. Eng. J. 384 (2020) 123265.
[32] Y. Wu, Y. Shi, H. Chen, J. Zhao, W. Dong, Process Saf. Environ. Prot. 116 (2018) 468–476.
[33] H. Gao, J. Chen, Y. Zhang, X. Zhou, Chem. Eng. J. 306 (2016) 522–530.
[34] S. Yang, P. Wang, X. Yang, et al., J. Hazard. Mater. 179 (2010) 552–558.
[35] N. Liu, F. Ding, C.H. Weng, C.C. Hwang, Y.T. Lin, J. Environ. Manag. 206 (2018) 565–576.
[36] C. Luo, J. Ma, J. Jiang, et al., Water Res. 80 (2015) 99–108.
[37] L. Wang, W. Liu, T. Wang, J. Ni, Chem. Eng. J. 225 (2013) 153–163.
[38] R. Li, J.J. Wang, B. Zhou, et al., Sci. Total Environ. 559 (2016) 121–129.
[39] H. Li, J. Wan, Y. Ma, Y. Wang, Z. Guan, RSC Adv. 5 (2015) 99935–99943.
[40] B. Lin, M. Hua, Y.Y. Zhang, et al., Chemosphere 166 (2017) 422–430.
[41] J. Luo, X. Luo, J. Crittenden, et al., Environ. Sci. Technol. 49 (2015) 11115–11124.
[42] M. Mallet, K. Barthelemy, C. Ruby, A. Renard, S. Naille, J. Colloid Interface Sci. 407 (2013) 95–101.